



# Optimizing Heat Dissipation in Microchannel Heat Sinks using Hybrid Nanofluids: A Computational Study

F. Nasiri Khamesloo, D. Domiri Ganji\*

Department of Mechanical Engineering, Babol Noshirvani University of Technology, Babol, Iran

## PAPER INFO

### Paper history:

Received 18 November 2023

Accepted in revised form 27 December 2023

### Keywords:

Heat sink  
Hybrid nanofluid  
Microchannel  
Numerical study

## ABSTRACT

The use of microchannel heat sinks is one of the most popular methods for cooling electronic components. In recent years, fractal microchannels have attracted researchers' attention, leading to increased heat transfer and reduced pressure drop compared to parallel microchannels. In this study, two hybrid nanofluids under laminar flow conditions are used for cooling inside microchannels, and simulations are conducted using COMSOL Multiphysics software. Parameters such as pumping power, maximum temperature, and performance evaluation coefficient are investigated for two hybrid nanofluids,  $\text{Fe}_3\text{O}_4\text{-MoS}_2$  and  $\text{Fe}_3\text{O}_4\text{-Al}_2\text{O}_3$  (mixed 50%-50% and with a volume fraction of 1% for each nanoparticle). The results indicate that the thermal performance of  $\text{Fe}_3\text{O}_4\text{-MoS}_2$  hybrid nanofluid is superior, leading to a 0.5% improvement in the maximum temperature of the heat sink. On the other hand, the use of this hybrid nanofluid increases pumping power by 9% inside the microchannel. Ultimately, the overall system performance is enhanced with the use of both hybrid nanofluids, and the  $\text{Fe}_3\text{O}_4\text{-MoS}_2$  hybrid nanofluid improves the overall system performance by 3.2%, providing better performance and making it more suitable for cooling microchannel heat sinks.

doi: 10.5829/ijee.2024.15.04.07

## NOMENCLATURE

$u_m$	Average velocity (m/s)	$k_s$	Thermal conductivity of solid (W/(m K))
$D_h$	Hydraulic diameter (mm)	$k_f$	Thermal conductivity of fluid (W/(m k))
$c_p$	Specific heat capacity (J/(kg K))	$Nu_{m,i}$	Nusselt number
$T_f$	Temperature of fluid (K)	<b>Greek Symbols</b>	
$T_s$	Temperature of the solid (K)	$\rho$	Density (kg/m <sup>3</sup> )
<b>Subscripts</b>		$\mu$	Dynamic viscosity (N*s/m <sup>2</sup> )
$f$	fluid	$\varphi$	Volume fraction
$hnf$	hybrid nanofluid		

## INTRODUCTION

Heat sinks function as heat exchangers in electronic devices and control the heat generated in electronic or mechanical chips. By absorbing and dissipating heat into the surrounding fluid, the heat sink prevents the temperature of the component from rising excessively

and protects it from damage. Heat sinks become particularly important when components are sensitive to temperature increases in the circuit or device. In recent decades, the development of Microelectromechanical Systems (MEMS) and nanotechnology has led to the advancement of compact and high-performance thermal systems for various applications such as electronics,

\*Corresponding Author Email: [ddg\\_davood@yahoo.com](mailto:ddg_davood@yahoo.com)  
(D. Domiri Ganji)

medical devices, high-power lasers, military electronics, and aerospace equipment. In these systems, thermal management poses a significant challenge, and the use of microchannel heat sinks is an effective method for addressing the heat dissipation issue.

Tuckerman and Pease (1) designed the first microchannel heat sink, laying the foundation for research and advancements in this field. Subsequently, extensive research has been conducted in this area. The concept of fractal bionic microchannels was first introduced by Bejan and Errera (2). They proposed a channel construction strategy based on structural theory to minimize flow resistance along the path. In two subsequent papers (3, 4), they explained the great potential of fractal bio-inspired microchannels by combining structural theory and the principle of entropy generation. Chen and Cheng (5) inspired by fractal patterns in mammalian circulatory and respiratory systems, presented a new design of branched fractal network channels (H-shaped) for cooling electronic chips. In their subsequent study (6), based on research results, they found that the H-shaped system performs best when the number of fractal branches is equal to 4. Pence (7) compared two microchannel heat sinks, one in a tree-like shape and the other in an H-shape, under the same conditions. The results showed that the overall performance of the tree-like microchannel was better than the other. Wang et al. (8) inspired by natural branching systems such as tree branches, leaves, root systems, river basins, mammalian circulatory and respiratory systems, proposed leaf-shaped networks for electronic component cooling. They compared the flow characteristics and heat transfer of symmetric and asymmetric leaf-shaped fractal networks. The results showed that an asymmetric structure can significantly reduce pressure drop while maintaining maximum temperature difference. Xu et al. (9) investigated the heat transfer performance in a fractal microchannel network made of silicon and cooled by water under pulsating flow, both experimentally and numerically. Yan et al. (10) designed and simulated a dual-objective thermal-hydraulic optimization model using ANSYS software, comparing it with hydraulic and thermal optimization models. The results showed that a microchannel with 15 main branches had the best overall performance. In another paper (11), they used thermally responsive hydrogels to control mass flow rate in a fractal microchannel heat sink for addressing localized hot spot failures in electronic chips, which enhanced cooling efficiency in the hot spot areas. Jalili et al. (12) investigate the heat transfer of nanofluid flow through a microchannel heat sink in the presence of a magnetic field. The results show that applying a magnetic field correlates with the Nusselt number, and heat transfer increases with higher nanofluid concentration up to 0.04.

Nanofluid is a new type of fluid that is made by dispersing nanoscale materials such as nanoparticles, nanotubes, and nanowires in a base fluid. The use of

nanoparticles increases the thermal conductivity of the base fluid, which is why nanofluids are used to enhance heat transfer. Hybrid nanofluids are a new generation of nanofluids that are composed of a combination of different types of nanoparticles. Increasing heat transfer and reducing pressure drop are fundamental challenges in the use of nanofluids. Therefore, the use of hybrid nanofluids is important because it allows for the selection of two nanoparticles that can create desirable properties when combined. The first use of nanofluids for heat transfer enhancement was reported by Choi and Eastman (13). Koblinski et al. (14) discovered through studies on nanofluids that thermal conductivity increases with decreasing particle size. Ho and Chen (15) experimentally investigated forced convective heat transfer using water- $\text{Al}_2\text{O}_3$  nanofluid in a mini-channel copper heat sink. Pourfattah et al. (16) simulated heat transfer and flow characteristics of water-CuO nanofluid under laminar flow regime in a microchannel heat sink and compared the results with available experimental data from other articles. They examined the effects of inlet-to-outlet ratio, Reynolds number, and solid nanoparticle concentration as independent parameters on heat transfer and flow field characteristics. Lyu et al. (17) studied the thermal performance of single-walled carbon nanotubes (SWCNT) and multi-walled carbon nanotubes (MWCNT) dispersed in two base fluids, water and kerosene, in a fractal microchannel at Reynolds numbers ranging from 1500 to 3000. The results showed that the use of a fractal silicon microchannel led to a uniform temperature distribution. Ghadikolaei et al. (18) investigate natural convection heat transfer of a non-Newtonian Carreau nanofluid with  $\text{TiO}_2$ -CuO hybrid nanoparticles in an ethylene glycol-water mixture over a rotating cone. The study analyzes the effects of various parameters on velocity and temperature profiles, skin friction coefficient, and local Nusselt number, highlighting the significant influence of hybrid nanoparticles on the temperature profile. Jalili et al. (19, 20) used analytical techniques to study forced convection heat transfer in nanofluids and non-Newtonian fluids, examining effects of parameters on velocity, temperature, and nanoparticle profiles. The methods effectively model heat transfer, with nanoparticles enhancing heat transfer and parameters like magnetic field and Reynolds number impacting flow and temperature. Hosseinzadeh et al. (21) investigate the flow of a mixture of water and ethylene glycol with hybrid nanoparticles over a vertically stretching cylinder, considering the effects of various parameters and shape factors. The results reveal significant differences in shape factors and a reduction in radial velocity with increasing Hartmann number for the hybrid nanoparticles. Jalili et al. (22) compared three methods for simulating thermal diffusivity in a stenosis artery with a hybrid nanofluid. The results showed Akbari-Ganji Method is more accurate than Finite Element and Runge-Kutta methods, and by increasing

$\text{Al}_2\text{O}_3$  nanoparticle volume fraction reduces maximum temperature. Mahmoudi et al. (23) present a novel multigeneration system integrating a nanofluid-based parabolic trough collector with a quadruple-effect absorption refrigeration cycle, thermoelectric generator, PEM electrolyzer, vapor generator, and domestic water heater, examining the impact of various parameters on system performance, revealing 18.78 kW power generation, 82.21% collector energy efficiency, and insights into exergy destruction and COPs for the absorption chiller. Habibzadeh et al. (24) present a renewable energy system integrating solar and geothermal sources with nanofluid-based collectors, employing  $\text{SiO}_2$  and  $\text{TiO}_2$  nanoparticles, and evaluate their performance based on energy, exergy, and cost analysis, noting the impact of key parameters like solar irradiation and collector inlet temperature on efficiencies and hydrogen and freshwater production rates. There have been numerous valuable studies conducted in the fields of fluid mechanics, nanofluids, and microchannels, which are reported in the literature (25–34). These studies can serve as valuable resources for future research and advancements in these areas.

In the present study, fluid flow and heat transfer in a fractal microchannel heat sink have been simulated using COMSOL Multiphysics software. The choice of a fractal structure is motivated by its high heat transfer capabilities and lower pumping power compared to parallel microchannel configurations. The fractal microchannel investigated in this research, with 15 branches, has been proposed by scientists in recent years and represents the optimal thermohydraulic configuration. Given that, in this specific geometry, hybrid nanofluids have not been previously explored, and considering the necessity to enhance heat transfer in heat sinks to prevent chip temperature rise, two hybrid nanofluids,  $\text{Fe}_3\text{O}_4\text{-MoS}_2$  and  $\text{Fe}_3\text{O}_4\text{-Al}_2\text{O}_3$  (a 50%-50% mixture with a volume fraction of 1% for each nanoparticle), are used as the cooling fluid. These hybrid nanofluids are compared with a base fluid of water. The selection of  $\text{Fe}_3\text{O}_4\text{-MoS}_2$  and  $\text{Fe}_3\text{O}_4\text{-Al}_2\text{O}_3$  hybrid nanofluids is based on their potential to improve overall microchannel fractal performance. The hybrid nanofluids are evaluated hydrodynamically and thermally, considering parameters such as pumping power and Nusselt number. Ultimately, through the investigation of various parameters, the best-performing nanofluid is proposed to enhance the overall performance of the fractal microchannel.

## PROBLEM STATEMENT

### Physical model

In the present study, fluid flow and heat transfer within a fractal microchannel heat sink will be investigated in the presence of two hybrid nanofluids using numerical

simulations in software. The application of numerical methods provides the flexibility to adjust problem conditions, including boundary conditions and various parameters, in accordance with the physics and geometry of the problem. The disc-shaped microchannel heat sink under investigation in this research has been introduced by Yan (10) and collaborators. Fractal microchannels, inspired by fractal patterns found in the circulatory and respiratory systems of mammals, are designed with characteristics such as increased heat transfer efficiency and reduced pumping power compared to traditional microchannels. The specific fractal microchannel studied in this research represents an optimal thermo-hydraulic configuration, as illustrated in Figure 1. Although this microheat sink features 15 main branches, as depicted in Figure 1, for computational convergence and efficiency improvement, a one-fifteenth structure of the entire microheat sink, as shown in Figure 2, is considered for numerical simulation. The COMSOL Multiphysics software, known for its capabilities in fluid mechanics, has been employed for numerical simulations. Given COMSOL's ability to import geometry from Computer-Aided Design (CAD) software, the simulation geometry was designed using SolidWorks and then imported into the COMSOL software. The geometry under investigation includes a central inlet within a sector and eight outlet orifices along the periphery, as outlined in Figure 2. The overall radius of the geometry is 11 millimeters, with a 1-millimeter radius for the inlet orifice, a 0.2-millimeter channel bed height, and a 0.5-millimeter channel height. Heat flux is introduced into the microchannel from below, and fluid flow within the microchannel facilitates heat transfer.

The important feature of nanoparticles is the enhancement of heat transfer. The use of nanoparticles can improve the thermal performance of the system, a subject not addressed in the fractal microchannel heat sink. Hybrid nanofluids are a new generation of nanofluids formed by the combination of different nanoparticles. Enhancing heat transfer and reducing pumping power are fundamental challenges of nanofluid utilization. Therefore, the use of hybrid nanofluids is significant as it allows the selection of two nanoparticles

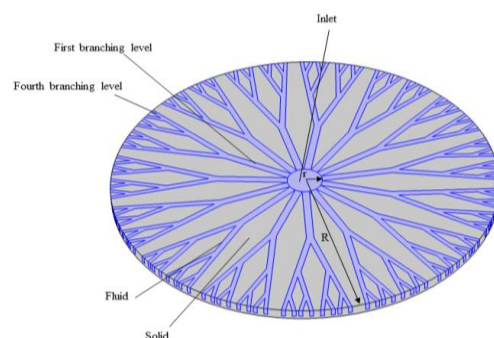


**Figure 1.** The primary geometry of MCHS

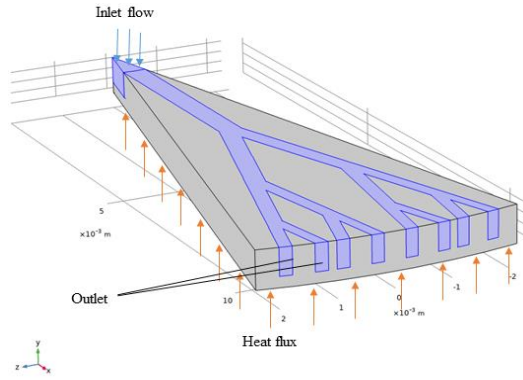


Figure 2. One fifteenth of the main geometry

that, together, create desirable properties. In this study, two hybrid nanofluids,  $Fe_3O_4-MoS_2$  and  $Fe_3O_4-Al_2O_3$  (50%-50%) with a volume fraction of 1% for each nanoparticle, were used as the coolant fluid, and comparison was made with the base fluid, water. The COMSOL software was employed, utilizing two physics: heat transfer in the fluid-solid and laminar flow, for numerical simulation. After simulation, various parameters, including temperature distribution, pumping power, and the heat sink's performance coefficient, were investigated within an input flow rate range of 200 to 400 mL/min and a constant heat flux of  $100 \text{ W/cm}^2$ .

### Numerical model

The properties of hybrid nanofluids have been calculated using the following equations (35):

The viscosity of hybrid nanofluids for spherical nanoparticles can be estimated as:

$$\mu_{hnf} = \frac{\mu_f}{(1-\phi_1)^{2.5} \times (1-\phi_2)^{2.5}} \quad (1)$$

The density and specific heat capacity of a hybrid nanofluid with any shape of nanoparticle can be obtained from the following equations:

$$\rho_{hnf} = \rho_f(1 - \phi_2) \left( (1 - \phi_1) + \phi_1 \left( \frac{\rho_{s1}}{\rho_f} \right) \right) + \phi_2 \rho_{s2} \quad (2)$$

$$(\rho c_p)_{hnf} = (\rho c_p)_f(1 - \phi_2) \left( (1 - \phi_1) + \phi_1 \frac{(\rho c_p)_{s1}}{(\rho c_p)_f} \right) + \phi_2 (\rho c_p)_{s2} \quad (3)$$

The effective thermal conductivity coefficient of a hybrid nanofluid can be approximately obtained from the following equations:

$$k_{bf} = k_f \times \left( \frac{k_{s1} + (s-1)k_f - (s-1)\phi_1(k_f - k_{s1})}{k_{s1} + (s-1)k_f + \phi_1(k_f - k_{s1})} \right) \quad (4)$$

$$k_{hnf} = k_{bf} \times \left( \frac{k_{s2} + (s-1)k_{bf} - (s-1)\phi_2(k_{bf} - k_{s2})}{k_{s2} + (s-1)k_{bf} + \phi_2(k_{bf} - k_{s2})} \right)$$

The thermophysical properties of nanoparticles and the base fluid are presented in Table 1.

Fluid behavior in a control volume is described using the Navier-Stokes equations (10), which are expressed as: Continuity equation: To investigate the conservation of mass, the continuity equation is used in the following form:

$$\nabla \cdot \vec{v} = 0 \quad (5)$$

Momentum equation:

$$\rho(\vec{v} \cdot \nabla \vec{v}) = -\nabla p + \mu \cdot \nabla^2 \vec{v} \quad (6)$$

Energy equation for fluid:

$$\rho c_p(\vec{v} \cdot \nabla T_{hnf}) = k_{hnf} \nabla^2 T_{hnf} \quad (7)$$

Energy equation for solid:

$$k_s \nabla^2 T_s = 0 \quad (8)$$

In given equations,  $\vec{v}$  represents the velocity,  $\rho$  denotes the density of the coolant fluid,  $\vec{p}$  represents the hydrodynamic pressure,  $\mu$  corresponds to the viscosity of the hybrid nanofluid,  $c_p$  represents the specific heat capacity of the hybrid nanofluid,  $T_{hnf}$  represents the temperature of the hybrid nanofluid,  $k_{hnf}$  denotes the thermal conductivity coefficient of the hybrid nanofluid, and  $k_s$  and  $T_s$  respectively represent the thermal conductivity coefficient and temperature of the solid section.

The following parameters are used to evaluate the efficacy of a MCHS:

Pumping power:

$$W_{pump} = \Delta P_{tot} \times q_v \quad (9)$$

where  $\Delta P_{tot}$  represents the total pressure drop and  $q_v$  denotes the volumetric flow rate.

Average Re in each branch:

$$Re_{m,i} = \frac{\rho \times u_{m,i} \times D_h}{\mu} \quad (10)$$

Average Nusselt number in each branch:

$$Nu_{m,i} = \frac{q \times D_{h,i}}{k_f \times (T_{m,wi} - T_{m,fi})} \quad (11)$$

$D_h$  represents the hydraulic diameter,  $q$  denotes the heat flux. Additionally,  $T_{m,wi}$  and  $T_{m,fi}$  respectively indicate

Table 1. Thermodynamic Properties (36)

Thermodynamic properties		$\rho$ (kg/m <sup>3</sup> )	$c_p$ (J/kgK)	$k$ (W/mK)
Base fluid	Water	997.1	4179	0.613
Nanoparticles	$Fe_3O_4$	5180	670	9.7
	$Al_2O_3$	3970	765	40
	$MoS_2$	5060	397.21	904.4

the average wall temperature and the bulk fluid temperature.

Friction factor:

$$f = 2\Delta P \frac{D_h}{L} \frac{1}{\rho u_{in}^2} \quad (12)$$

Performance evaluation criterion:

$$PEC = \frac{\left(\frac{Nu_{ave}}{Nu_{ave,\varphi=0}}\right)}{\left(\frac{f}{f_{\varphi=0}}\right)^{\frac{1}{3}}} \quad (13)$$

**Boundary conditions**

The boundary conditions are specified based on Figure 2. The fluid flow is steady, laminar, and incompressible, and the fluid properties are assumed to be constant at the operating temperature. The inlet temperature is 293.15 K, the inlet flow rate ranges from 200 to 400 mL/min, and the outlet pressure is set equal to atmospheric pressure. The heat sink is made of copper and is insulated from the surrounding environment. A heat flux of 100 W/cm<sup>2</sup> is applied to the bottom wall of the heat sink. No-slip conditions are enforced on the walls, and the effects of radiation and gravity are neglected. Due to simulating a one-fifteenth portion of the original geometry, the symmetry boundary condition is applied to the lateral walls of the sector.

**Grid independence**

During the numerical solution process in software, grid or mesh generation plays a pivotal role. The accuracy of calculations heavily relies on creating an appropriate grid, as it impacts both the computational cost and the precision of the simulation. To achieve accurate results while maintaining computational efficiency, the grid must strike a balance between being fine enough to capture key features and not excessively refined. Specifically, near walls and edges where flow variables exhibit significant gradients, finer meshes are needed to ensure high accuracy. Conversely, the grid in the solid region can have a coarser resolution compared to the liquid region.

To assess result accuracy, the maximum temperature and pressure drop were analyzed for five different grid generations: 384,063; 678,638; 913,416; 1,324,415; and 1,693,398 grids. The findings indicate that from the third grid onwards, the changes in the maximum temperature and pressure drop become negligible. Consequently, a mesh consisting of 913,416 grids has been selected as the optimal choice to proceed with the simulation process. The graph illustrating the variations in maximum temperature with an increase in mesh is presented in Figure 3.

**Validation**

To validate the accuracy of the simulation, the computed pumping power has been compared with the pumping power-flow rate relationship presented in Yan's article

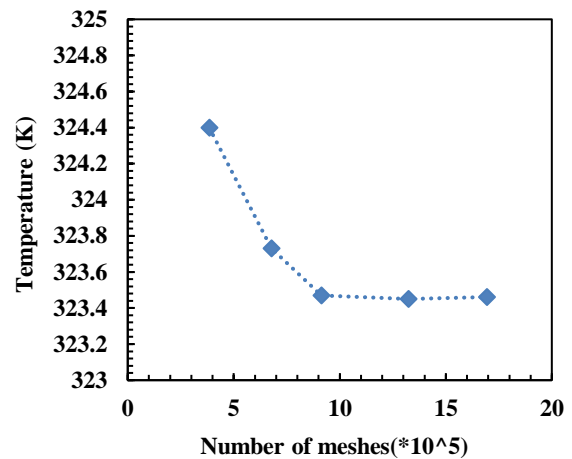


Figure 3. Temperature Variation with Mesh Changes

(10). The validation process involves using water as the coolant fluid and applying a heat flux of 50 W/cm<sup>2</sup>. Figure 4 illustrates the comparison between the obtained results and the data provided in the referenced article, demonstrating a satisfactory agreement between the two datasets. The obtained results indicate a 6% difference compared to Yan's article.

**RESULTS AND DISCUSSION**

The aim of this study is to investigate the thermal performance of a microchannel heat sink under laminar flow. Two hybrid nanofluids, Fe<sub>3</sub>O<sub>4</sub>-MoS<sub>2</sub> and Fe<sub>3</sub>O<sub>4</sub>-Al<sub>2</sub>O<sub>3</sub> (50%-50%), are used for cooling the microchannel heat sink and compared with water to determine the effect of the hybrid nanofluids and identify the best hybrid nanofluid for cooling and future applications. The primary objective of using a heat sink is to reduce the maximum temperature in temperature-sensitive components. Therefore, the maximum temperature of the

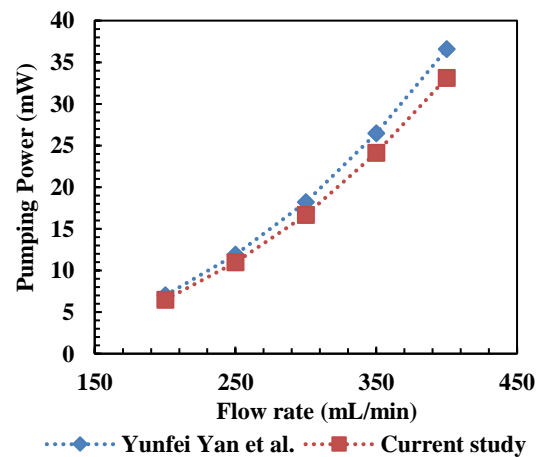


Figure 4. Model validation

heat sink during operation is of particular importance, as a lower value ensures system performance. Figure 5 presents the maximum temperatures in three conditions for water and the hybrid nanofluids  $\text{Fe}_3\text{O}_4\text{-MoS}_2$  and  $\text{Fe}_3\text{O}_4\text{-Al}_2\text{O}_3$ . As shown in Figure 5, with an increase in the inlet mass flow rate, the maximum temperature of the heat sink exhibits a decreasing trend. This is due to the improved heat transfer between the coolant fluid and the microchannel wall as a result of the increased flow rate and velocity. Furthermore, the addition of hybrid nanofluids to water enhances the thermal conductivity, which leads to increased heat transfer and reduced heat sink temperature. The lower temperature observed when using  $\text{Fe}_3\text{O}_4\text{-MoS}_2$  hybrid nanofluid as the coolant is attributed to its higher thermal conductivity compared to the other two conditions. The maximum temperature of the heat sink at a mass flow rate of 400 mL/min for water,  $\text{Fe}_3\text{O}_4\text{-MoS}_2$ , and  $\text{Fe}_3\text{O}_4\text{-Al}_2\text{O}_3$  hybrid nanofluids is 337.18 K, 335.88 K, and 336.1 K, respectively.

Figure 6 illustrates the temperature contour at a mass flow rate of 200 mL/min for the three discussed conditions. As evident from Figure 6, there is a slight improvement in the temperature distribution within the heat sink when using hybrid nanofluids compared to the base case with water as the coolant. It can be observed that the highest temperatures occur at points further away from the microchannels, while lower temperatures are observed in proximity to the microchannels due to heat exchange between the fluid and the walls.

Figure 7 presents the temperature contour at different mass flow rates for the  $\text{Fe}_3\text{O}_4\text{-MoS}_2$  hybrid nanofluid. As evident from the figure, as the mass flow rate increases, the temperature distribution within the heat sink becomes more uniform, and the temperature gradient is reduced. With an increase in the mass flow rate and inlet velocity of the  $\text{Fe}_3\text{O}_4\text{-MoS}_2$  hybrid nanofluid, heat exchange between the walls and the fluid improves, leading to a reduction in the heat sink temperature.

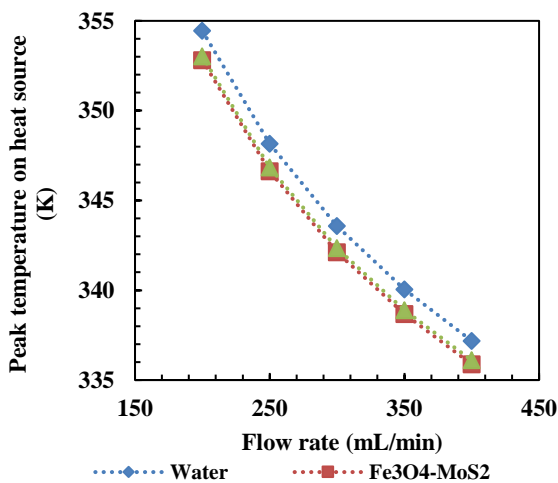


Figure 5. Maximum temperature in the heat sink

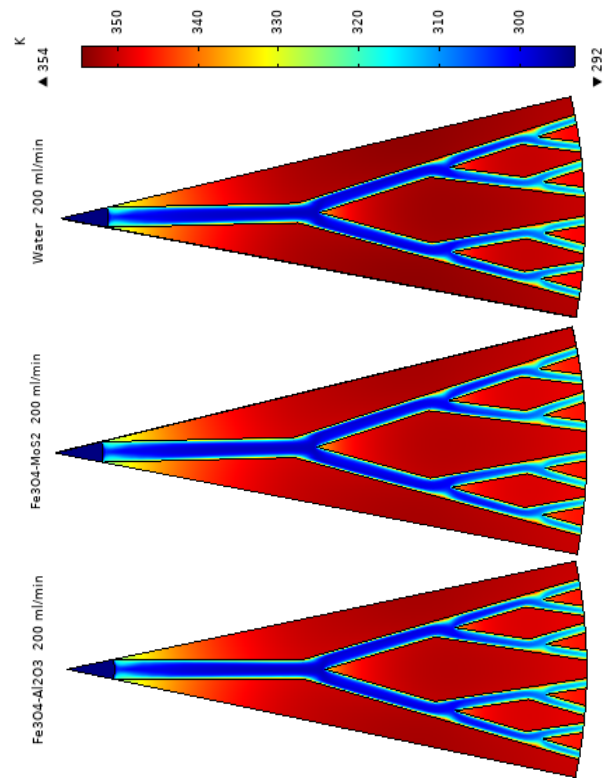


Figure 6. Temperature distribution in heat sink

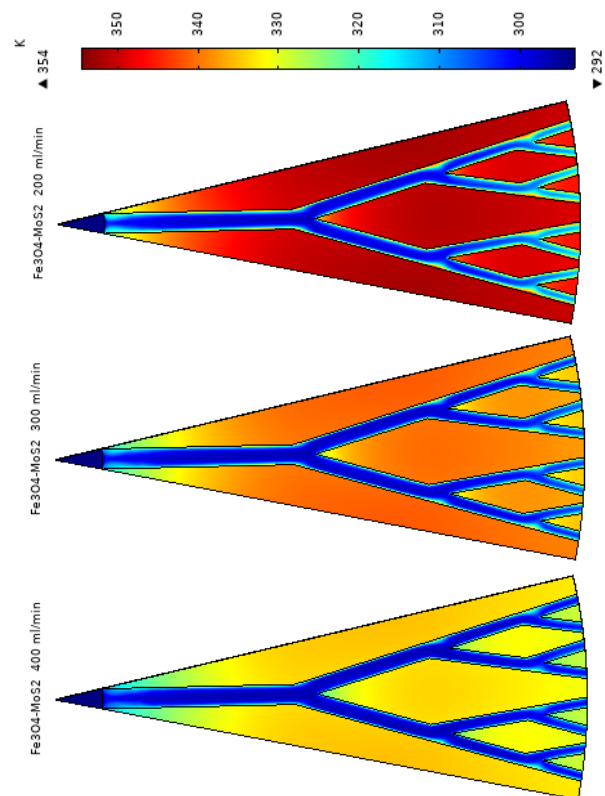


Figure 7. Temperature contour for the  $\text{Fe}_3\text{O}_4\text{-MoS}_2$

Figure 8 compares the pumping power for the three different microchannel heat sink configurations. The highest pumping power belongs to the Fe<sub>3</sub>O<sub>4</sub>-MoS<sub>2</sub> hybrid nanofluid, followed by the Fe<sub>3</sub>O<sub>4</sub>-Al<sub>2</sub>O<sub>3</sub> hybrid nanofluid and water. The pumping power is influenced not only by geometric parameters but also by thermophysical properties such as viscosity, density, and inlet velocity. By adding hybrid nanoparticles to water, the density and viscosity of the fluid increase, leading to an increase in overall pressure drop and consequently increasing the pumping power of the microchannel. Essentially, the hybrid nanofluid becomes denser and requires more pumping power to flow through the microchannels. As observed from the graph, the pumping power of the two hybrid nanofluids is very close to each other, which can be attributed to their similar thermodynamic properties. Additionally, as shown in the graph, the pumping power increases with an increasing inlet mass flow rate. This is because when the inlet mass flow rate is higher, the collision between the hybrid nanoparticles and the microchannel walls becomes more intense, resulting in higher forces exerted by the walls on the nanoparticles, leading to an increased pressure drop.

In order to better understand and analyze the fluid flow inside a microchannel heat sink, both positive and negative aspects need to be simultaneously evaluated. Therefore, thermal and hydraulic parameters should be investigated concurrently to determine their impact on the overall system performance. For example, adding nanoparticles or altering the geometric shape of the microchannel can enhance heat transfer within the microchannel, but it can also lead to a significant increase in pressure drop, thereby reducing the overall system performance. Equation 13 is defined for this reason, to enable the simultaneous evaluation of thermal and hydraulic performance.

Figure 9 depicts the performance evaluation coefficient for two hybrid nanofluids. As evident, for both

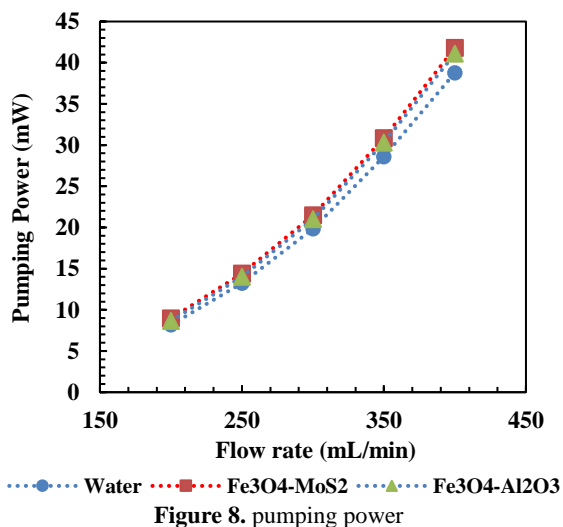


Figure 8. pumping power

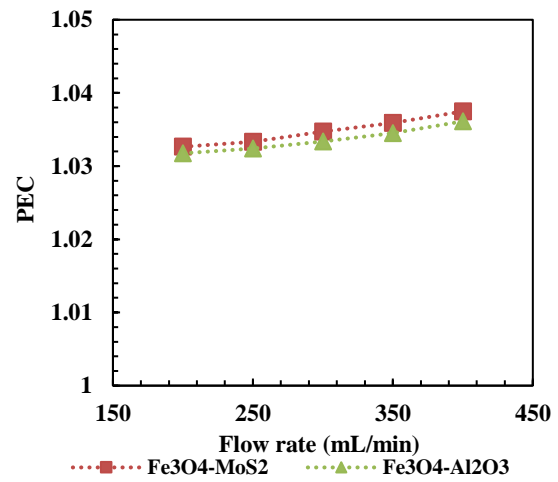


Figure 9. PEC for two new hybrid nanofluids

hybrid nanofluids, this coefficient is above 1, indicating that both hybrid nanofluids enhance the overall system performance. It is also evident that the performance evaluation coefficient increases with increasing flow rate, suggesting that higher flow rates should be employed for cooling the heat sink. Based on the graph, it is evident that the Fe<sub>3</sub>O<sub>4</sub>-MoS<sub>2</sub> hybrid nanofluid has a higher performance evaluation coefficient compared to the Fe<sub>3</sub>O<sub>4</sub>-Al<sub>2</sub>O<sub>3</sub> hybrid nanofluid, thus providing a greater enhancement in the overall system performance. However, the difference in this value between the two hybrid nanofluids is relatively small.

Based on the above information, it can be concluded that the Fe<sub>3</sub>O<sub>4</sub>-MoS<sub>2</sub> hybrid nanofluid improves the overall system performance to a greater extent, and it is preferable to utilize this hybrid nanofluid for cooling purposes.

## CONCLUSION

A microchannel heat sink is one of the best methods for cooling in industry and electronic systems. In this research, a microchannel heat sink has been numerically investigated using COMSOL Multiphysics software. The software utilizes heat transfer physics in fluid-solid and laminar flow in three dimensions. Two hybrid nanofluids, Fe<sub>3</sub>O<sub>4</sub>-MoS<sub>2</sub> and Fe<sub>3</sub>O<sub>4</sub>-Al<sub>2</sub>O<sub>3</sub>, are used for cooling and compared with water as the base fluid. The overall goal is to compare the two hybrid nanofluids and their impact on fluid flow to select the best hybrid nanofluid for cooling in terms of overall performance. To comprehensively assess the thermal and hydraulic performance of the microchannel, the performance evaluation coefficient is calculated to identify the optimal condition, considering both thermal and hydraulic aspects. A summary of the results is provided below.

- The use of hybrid nanoparticles leads to an improvement in heat transfer, which is attributed to

the increased heat transfer coefficient when using nanoparticles. The maximum temperature of the heat sink when using water as a coolant at a flow rate of 200 milliliters per minute is 354.44°C. However, this value decreases when using hybrid nanofluids. For the Fe<sub>3</sub>O<sub>4</sub>-MoS<sub>2</sub> and Fe<sub>3</sub>O<sub>4</sub>-Al<sub>2</sub>O<sub>3</sub> hybrid nanofluids, the maximum temperatures are 352.8°C and 353.02°C, respectively, indicating a slight improvement compared to the base case. The use of hybrid nanofluids Fe<sub>3</sub>O<sub>4</sub>-MoS<sub>2</sub> and Fe<sub>3</sub>O<sub>4</sub>-Al<sub>2</sub>O<sub>3</sub> leads to an improvement of 0.46% and 0.4% in the maximum temperature of the heat sink, respectively.

- While the use of nanofluids improves heat transfer, it also leads to an increase in pressure drop and, consequently, an increase in pumping power. This can be attributed to the increased viscosity and density of the fluid flow. The pumping power for water at a flow rate of 200 milliliters per minute is 8.17 mW. However, for the Fe<sub>3</sub>O<sub>4</sub>-MoS<sub>2</sub> and Fe<sub>3</sub>O<sub>4</sub>-Al<sub>2</sub>O<sub>3</sub> hybrid nanofluids, the pumping powers are 8.94 and 8.65 mW, respectively. The use of hybrid nanofluids Fe<sub>3</sub>O<sub>4</sub>-MoS<sub>2</sub> and Fe<sub>3</sub>O<sub>4</sub>-Al<sub>2</sub>O<sub>3</sub> results in an increase of 9% and 6% in the pumping power, respectively. The results indicate that although the heat transfer performance of the Fe<sub>3</sub>O<sub>4</sub>-MoS<sub>2</sub> hybrid nanofluid is better than the other one, its pumping power is also higher.
- By examining the Performance Evaluation Coefficient (PEC) for both hybrid nanofluids, it has been determined that both nanofluids improve the overall system performance, and the overall system performance further improves with increasing inlet flow rate. The Fe<sub>3</sub>O<sub>4</sub>-MoS<sub>2</sub> hybrid nanofluid enhances the overall system performance by 3.2% at a flow rate of 200 milliliters per minute, while the other hybrid nanofluid improves it by 3.1%. Therefore, it is better to utilize the Fe<sub>3</sub>O<sub>4</sub>-MoS<sub>2</sub> hybrid nanofluid based on these results.

### Suggestions

For future work, the following options may be helpful for researchers interested in working in this field:

- Investigation of two-layer and multilayer microchannels and their effects on the overall system performance.
- Examination of incorporating fins inside microchannels to enhance heat transfer.
- Study of heat transfer under non-uniform heat flux conditions.
- Exploration of non-rectangular geometries for microchannels and their impact on improving heat sink performance.
- Research on microchannels in turbulent flow regimes at different Reynolds numbers.

### REFERENCES

1. Tuckerman DB, Pease RFW. High-Performance Heat Sinking for VLSI. *IEEE Electron Device Letters*. 1981;EDL-2(5):126–9. Doi: 10.1109/edl.1981.25367.
2. Bejan A, Errera MR. Deterministic tree networks for fluid flow: Geometry for minimal flow resistance between a volume and one point. *Fractals*. 1997;5(4):685–95. Doi: 10.1142/s0218348x97000553.
3. Bejan A. From heat transfer principles to shape and structure in nature: Constructal theory. *Journal of Heat Transfer*. 2000;122(3):430–49. Doi: 10.1115/1.1288406.
4. Bejan A, Lorente S. Constructal theory of generation of configuration in nature and engineering. *Journal of Applied Physics*. 2006;100(4). Doi: 10.1063/1.2221896.
5. Chen Y, Cheng P. Heat transfer and pressure drop in fractal tree-like microchannel nets. *International Journal of Heat and Mass Transfer*. 2002;45(13):2643–8. Doi: 10.1016/s0017-9310(02)00013-3.
6. Chen Y, Cheng P. An experimental investigation on the thermal efficiency of fractal tree-like microchannel nets. *International Communications in Heat and Mass Transfer*. 2005;32(7):931–8. Doi: 10.1016/j.icheatmasstransfer.2005.02.001.
7. Pence D. Reduced pumping power and wall temperature in microchannel heat sinks with fractal-like branching channel networks. *Microscale Thermophysical Engineering*. 2003;6(4):319–30. Doi: 10.1080/10893950290098359.
8. Wang XQ, Xu P, Mujumdar AS, Yap C. Flow and thermal characteristics of offset branching network. *International Journal of Thermal Sciences*. 2010;49(2):272–80. Doi: 10.1016/j.ijthermalsci.2009.07.019.
9. Xu S, Wang W, Fang K, Wong CN. Heat transfer performance of a fractal silicon microchannel heat sink subjected to pulsation flow. *International Journal of Heat and Mass Transfer*. 2015;81:33–40. Doi: 10.1016/j.ijheatmasstransfer.2014.10.002.
10. Yan Y, Yan H, Yin S, Zhang L, Li L. Single/multi-objective optimizations on hydraulic and thermal management in micro-channel heat sink with bionic Y-shaped fractal network by genetic algorithm coupled with numerical simulation. *International Journal of Heat and Mass Transfer*. 2019;129:468–79. Doi: 10.1016/j.ijheatmasstransfer.2018.09.120.
11. Yan Y, He Z, Wu G, Zhang L, Yang Z, Li L. Influence of hydrogels embedding positions on automatic adaptive cooling of hot spot in fractal microchannel heat sink. *International Journal of Thermal Sciences*. 2020;155. Doi: 10.1016/j.ijthermalsci.2020.106428.
12. Jalili B, Rezaeian A, Jalili P, Omidi F, Domiri Ganji D. Numerical modeling of magnetic field impact on the thermal behavior of a microchannel heat sink. *Case Studies in Thermal Engineering*. 2023;45. Doi: 10.1016/j.csite.2023.102944.
13. Choi SUS, Eastman JA. Enhancing thermal conductivity of fluids with nanoparticles. Argonne National Lab.(ANL), Argonne, IL (United States); 1995.
14. Keblinski P, Phillpot SR, Choi SUS, Eastman JA. Mechanisms of heat flow in suspensions of nano-sized particles (nanofluids). *International Journal of Heat and Mass Transfer*. 2001;45(4):855–63. Doi: 10.1016/s0017-9310(01)00175-2.
15. Ho CJ, Chen WC. An experimental study on thermal performance of Al<sub>2</sub>O<sub>3</sub>/water nanofluid in a minichannel heat sink. *Applied Thermal Engineering*. 2013;50(1):516–22. Doi: 10.1016/j.applthermaleng.2012.07.037.
16. Pourfattah F, Abbasian Arani AA, Babaie MR, Nguyen HM, Asadi A. On the thermal characteristics of a manifold microchannel heat sink subjected to nanofluid using two-phase flow simulation. *International Journal of Heat and Mass Transfer*.



- 2019;143. Doi: 10.1016/j.ijheatmasstransfer.2019.118518.
17. Lyu Z, Pourfattah F, Arani AAA, Asadi A, Foong LK. On the Thermal Performance of a Fractal Microchannel Subjected to Water and Kerosene Carbon Nanotube Nanofluid. *Scientific Reports*. 2020;10(1). Doi: 10.1038/s41598-020-64142-w.
  18. Ghadikolaie SS, Hosseinzadeh K, Ganji DD. Investigation on ethylene glycol-water mixture fluid suspended by hybrid nanoparticles (TiO<sub>2</sub>-CuO) over rotating cone with considering nanoparticles shape factor. *Journal of Molecular Liquids*. 2018;272:226–36. Doi: 10.1016/j.molliq.2018.09.084.
  19. Jalili B, Ganji AM, Shateri A, Jalili P, Domiri Ganji D. Thermal analysis of Non-Newtonian visco-inelastic fluid MHD flow between rotating disks. *Case Studies in Thermal Engineering*. 2023;49. Doi: 10.1016/j.csite.2023.103333.
  20. Jalili P, Shateri A, Ganji AM, Jalili B, Ganji DD. Analytical analyzing mixed convection flow of nanofluid in a vertical channel using python approach. *Results in Physics*. 2023;52. Doi: 10.1016/j.rinp.2023.106908.
  21. Hosseinzadeh K, Asadi A, Mogharrebi AR, Ermia Azari M, Ganji DD. Investigation of mixture fluid suspended by hybrid nanoparticles over vertical cylinder by considering shape factor effect. *Journal of Thermal Analysis and Calorimetry*. 2021;143(2):1081–95. Doi: 10.1007/s10973-020-09347-x.
  22. Jalili P, Sadeghi Ghahare A, Jalili B, Domiri Ganji D. Analytical and numerical investigation of thermal distribution for hybrid nanofluid through an oblique artery with mild stenosis. *SN Applied Sciences*. 2023;5(4). Doi: 10.1007/s42452-023-05312-z.
  23. Mahmoudi M, Mirzaee I, Khalilian M. Energy and Exergy Study of a Nanofluid-based Solar System Integrated with a Quadruple Effect Absorption Cycle and Thermoelectric Generator. *Iranica Journal of Energy and Environment*. 2024;15(1):80–90. Doi: 10.5829/ijee.2024.15.01.08.
  24. Habibzadeh A, Abbasalizadeh M, Mirzaee I, Jafarmadar S, Shirvani H. Thermodynamic Modeling and Analysis of a Solar and Geothermal-driven Multigeneration System Using TiO<sub>2</sub> and SiO<sub>2</sub> Nanoparticles. *Iranian Journal of Energy and Environment*. 2023;14(2):127–38. Doi: 10.5829/ijee.2023.14.02.05.
  25. Zamani M, Shafaghat R, Alizadeh Kharkeshi B. Enhancing Performance Evaluation of Archimedes Screw Turbines under Optimal Conditions: A Focus on Flow Rate Analysis, Empirical Equations, and Comparative Scaling Methods. *Iranica Journal of Energy and Environment*. 2024;15(2):123–34. Doi: 10.5829/ijee.2024.15.02.01.
  26. Zamani M, Shafaghat R, Kharkeshi BA. Numerical Study of the Hydrodynamic Behavior of an Archimedes Screw Turbine by Experimental Data in order to Optimize Turbine Performance: The Genetic Algorithm. *Journal of Applied and Computational Mechanics*. 2023;9(4):1060–75. Doi: 10.22055/jacm.2023.43137.4031.
  27. Jalili B, Mousavi A, Jalili P, Shateri A, Ganji DD. Thermal Analysis of Fluid Flow with Heat Generation for Different Logarithmic Surfaces. *International Journal of Engineering Transactions C: Aspects*. 2022;35(12):1184–91. Doi: 10.5829/ijee.2022.35.12c.03.
  28. Jalili P, Afifi MD, Jalili B, Mirzaei AM, Ganji DD. Numerical Study and Comparison of Two-dimensional Ferrofluid Flow in Semi-porous Channel under Magnetic Field. *International Journal of Engineering, Transactions A: Basics*. 2023;36(11):2087–101. Doi: 10.5829/ijee.2023.36.11b.13.
  29. Pasha P, Domiri-Ganji D. Hybrid Analysis of Micropolar Ethylene-glycol Nanofluid on Stretching Surface Mounted Triangular, Rectangular and Chamfer Fins by FEM Strategy and Optimization with RSM Method. *International Journal of Engineering, Transactions B: Applications*. 2022;35(5):845–54. Doi: 10.5829/ijee.2022.35.05b.01.
  30. Hedayati P, Ramiar A, Hedayati N. Analyzing the Impact of a Curved Stator on the Performance of a Savonius Wind Turbine using Computational Fluid Dynamics. *Iranica Journal of Energy and Environment*. 2024;15(3):279–86. Doi: 10.5829/ijee.2024.15.03.06.
  31. Nasiri Khamesloo F, Domiri Ganji D. Optimizing Heat Transfer in Microchannel Heat Sinks: A Numerical Investigation with Nanofluids and Modified Geometries. *International Journal of Engineering, Transaction B: Applications*. 2024;37(5):860–75. Doi: 10.5829/ijee.2024.37.05b.05.
  32. Hedayati Goodarzi N, Rahimi-Esbo M. Optimizing Hydrogen Production from Methanol Reformers by Temperature Variation and Feed Ratio Using CFD. *Iranica Journal of Energy and Environment*. 2024;15(2):194–200. Doi: 10.5829/ijee.2024.15.02.09.
  33. Yousefi A, Shafaghat R, Beykani M, Aghajani Afghan A, Seyyed Mostafa ST. Experimental Study to Investigate Effect of Pitch Ratio and Number of Blades on Hydrodynamic Performance of Surface Piercing Propellers. *Iranian Journal of Energy and Environment*. 2023;14(1):26–37. Doi: 10.5829/ijee.2023.14.01.04.
  34. Aghajani Afghan S, Shafaghat R, Aghajani Afghan A, Hosseinalipour SM. An Experimental Study to Apply an Absorption Refrigeration Cycle as a Dehumidifier in Humidification-Dehumidification Solar Desalination System. *Iranian Journal of Energy and Environment*. 2023;14(4):361–71. Doi: 10.5829/ijee.2023.14.04.06.
  35. Hosseinzadeh K, Roghani S, Mogharrebi AR, Asadi A, Ganji DD. Optimization of hybrid nanoparticles with mixture fluid flow in an octagonal porous medium by effect of radiation and magnetic field. *Journal of Thermal Analysis and Calorimetry*. 2021;143(2):1413–24. Doi: 10.1007/s10973-020-10376-9.
  36. Salehi S, Nori A, Hosseinzadeh K, Ganji DD. Hydrothermal analysis of MHD squeezing mixture fluid suspended by hybrid nanoparticles between two parallel plates. *Case Studies in Thermal Engineering*. 2020;21. Doi: 10.1016/j.csite.2020.100650.

#### COPYRIGHTS

©2024 The author(s). This is an open access article distributed under the terms of the Creative Commons Attribution (CC BY 4.0), which permits unrestricted use, distribution, and reproduction in any medium, as long as the original authors and source are cited. No permission is required from the authors or the publishers.



#### Persian Abstract

#### چکیده

استفاده از سینک حرارتی میکروکانالی یکی از محبوب‌ترین روش‌ها برای خنک‌کاری قطعات الکترونیکی است. در سال‌های اخیر میکروکانال‌های فرکتال مورد توجه محققین بوده است که باعث افزایش انتقال حرارت و کاهش افت فشار در مقایسه با میکروکانال‌های موازی می‌شوند. در مطالعه حاضر از دو نانوسیال هیبریدی تحت جریان رژیم آرام برای خنک‌کاری درون میکروکانال استفاده شده و در نرم‌افزار کامسول مولتی فیزیک مورد شبیه‌سازی قرار گرفته است. پارامترهایی مثل توان پمپاژ، دمای ماکزیمم و ضریب ارزیابی عملکرد برای دو نانوسیال هیبریدی  $Fe_3O_4-MoS_2$  و  $Fe_3O_4-Al_2O_3$  (مخلوط ۵۰٪-۵۰٪ و کسر حجمی ۱ درصد برای هر نانوذره) مورد بررسی قرار گرفت. نتایج نشان داد که عملکرد حرارتی نانوسیال هیبریدی  $Fe_3O_4-MoS_2$  بهتر از دیگری است و باعث بهبود ۰/۵ درصدی در دمای حداکثر سینک حرارتی شده است. از طرفی دیگر استفاده از این نانوسیال هیبریدی باعث افزایش ۹ درصدی توان پمپاژ درون میکروکانال نیز می‌شود. در نهایت عملکرد کلی سیستم با استفاده از هر دو نانوسیال هیبریدی بهبود پیدا کرده است و نانوسیال هیبریدی  $Fe_3O_4-MoS_2$  باعث بهبود ۳/۲ درصدی عملکرد کلی سیستم می‌شود که عملکرد بهتر را ارائه می‌دهد و برای خنک‌کاری سینک‌های حرارتی میکروکانالی مناسب‌تر است.